Crater Detection by a Boosting Approach

Ricardo Martins, Pedro Pina, Jorge S. Marques, and Margarida Silveira

***Abstract*—An approach to automatically detect impact craters on planetary surfaces is presented in this letter. It is built up from a boosting algorithm proposed by Viola and Jones (2004) whose simplicity combined with an original learning strategy leads to a fast and robust process with consistent results. The approach is validated with image data sets from Mars surface captured by the Mars Orbiter Camera onboard Mars Global Surveyor probe.**

***Index Terms*—Automatic detection, boosting, impact craters, learning, Mars.**

I. Introduction

IMPACT craters are an essential source of information about the geology of planets and their surface characteristics. The density of craters is closely related to the age of the surfaces, and its computation has been used to establish a chronology of the evolution of the terrains [1]. After the primordial manual countings, several attempts to create reliable methods for automated crater detection have been developed. These include diverse approaches such as the ones based on template matching methods [2]–[5], Hough transform [6]–[8], neural networks [9], [10], genetic algorithms [11], [12], mathematical morphology [13], and a combination of multiple techniques [14], [15]. Anyhow, although relevant contributions have been presented over the years, the degree of generalization of those methods is not yet totally satisfactory, since adjustments or modifications on some of their steps are always necessary to respond to differences on planetary surfaces. In particular, the wide range of crater dimensions (from a few meters to thousands of kilometers) with distinct conservation conditions (from very fresh and well contrasted to very old with eroded rims and filled or covered by other geological materials) occurring in quite diverse geomorphological settings has also made difficult the choice of adequate and unique parameters on the different automated approaches. Most of those diversified characteristics can be found within single images, like the region of about 115×115 km^2 of Mars as clearly shown in Fig. 1.

Thus, the nature and varied characteristics of occurrence of these structures on planetary surfaces demand a learning strategy that is able to adapt itself to every distinct situation.

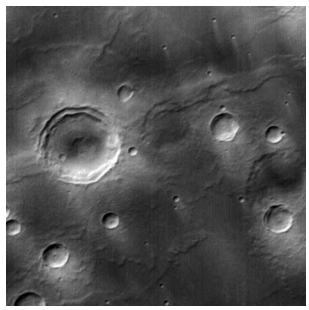

Fig. 1. Examples of impact craters and textural variation on the surface of Mars in a MOC image (M23-00337) with a spatial resolution of approximately 240 m/pixel (the side of the image is about 115 km) [image credits: NASA/JPL/MSSS].

These circumstances led us to explore a boosting approach whose dependence on the characteristics of the craters and the terrains where the impacts took place is reduced. This way, we decided to use a machine learning tool, the boosting algorithm proposed by Viola and Jones [16] in the context of face recognition. This algorithm is able to select a small number of useful features in face images, namely, the eyes and the mouth. The underlying idea follows the use of weak classifiers (simple thresholding operation applied to a single image feature) which are combined in an iterative procedure to create a strong classifier. We expect that it will also be able to extract meaningful characteristics of the craters' rims, although the problem is probably more difficult due to the great variety of textures.

This letter is organized as follows. Section II describes, in detail, the several steps of the crater detection algorithm. Section III introduces the strategy to deal with craters of different dimensions. Section IV presents the experimental results on a set of Martian images, while the conclusions of using this approach are presented in Section V.

II. Crater Detection

The detection of impact craters on planetary surfaces can be formulated as a classical pattern recognition problem where the information extracted from different locations in the images is assigned to one of two classes: crater or noncrater. A region or block around each image pixel is extracted to determine if it contains a crater or not; we will follow the approach used in [16] which achieved excellent results in the field of face recognition but which has not yet been applied in the context of crater detection. The decision (crater or noncrater) is given by a binary classifier using a set of image features; the classifier must deal with craters of different dimensions and with artifacts that may be confounded with the impact structures and which are produced by terrains of different constitutions

Manuscript received June 18, 2008; revised July 28, 2008. Current version published January 14, 2009. This work was supported in part by Fundação para a Ciência e a Tecnologia (Portugal) under Project PDCTE/CTA/49724/03 and in part by ISR/IST under pluriannual funding POSC, FEDER.

R. Martins is with the Instituto Superior Técnico, 1049-001 Lisboa, Portugal (e-mail: ricardo.martins@ist.utl.pt).

P. Pina is with the Instituto Superior Técnico, 1049-001 Lisboa, Portugal, and also with the Centro de Recursos Naturais e Ambiente, 1049-001 Lisboa, Portugal (e-mail: ppina@ist.utl.pt).

J. S. Marques and M. Silveira are with the Instituto Superior Técnico, 1049-001 Lisboa, Portugal, and also with the Instituto de Sistemas e Robótica, 1049-001 Lisboa, Portugal (e-mail: jsm@isr.ist.utl.pt; msilveira@isr.ist.utl.pt).

Digital Object Identifier 10.1109/LGRS.2008.2006004

Fig. 2. Five types of masks used for feature extraction.

and origins. Consequently, the issues to be taken into account in the design of a detection approach should rely on the selection and extraction of adequate features, on its classification, and on a strategy to achieve robustness with respect to scale changes (the first two issues are addressed in the following, while the third one is addressed separately in Section III).

A. Preprocessing

Planetary images have various lighting directions according to the relative position of the sun at the time of the capture of the image. Since the azimuth of the sun is known for each image, a rotation according to the registered value is executed in order to make sure that all images are aligned in the same lighting direction.

B. Feature Extraction

The features used in this letter are obtained by probing each image block B with the set of ternary masks (Haar-like features [17]) shown in Fig. 2. In these images, the gray tone stands for level 0 (region out of the mask), while the black and white regions stand for -1 and $+1$, respectively. Since we are looking for structures that may appear anywhere within the image block, we will consider the ternary masks at different positions. Let $\phi(x)$ denote one of these masks. The corresponding feature is given by

$$f(B) = \int_{[0,1]^2} B(x)\phi(x)dx \tag{1}$$

where we assumed that the block B and the masks are continuous images defined in the interval $[0,1]^2$. The computation of these features is extremely fast if an auxiliary image (integral image) is precomputed (see details on how to do it in [16]). By using the integral image, each feature can be obtained by a reduced number of additions (from four to eight). The number of generated features can attain a high value (typically thousands), but with distinct importances, from really relevant to absolutely irrelevant. Therefore, a selection of the most adequate features for this crater detection purpose must be performed.

C. Boosting Classifier [16]

The classification algorithm used in this letter is based on the variant of *AdaBoost* proposed by Viola and Jones [16]. This algorithm is used to select the features and to classify each block extracted from the image into one of two classes: crater or noncrater. First, a set of weak classifiers $\{h\}$ (one classifier per feature f) is defined, based on a thresholding operation

$$h(B) = \begin{cases} 1, & \text{if } p \cdot f(B) \geq p \cdot \theta \\ 0, & \text{otherwise} \end{cases} \tag{2}$$

where θ is a threshold and $p \in \{-1, 1\}$ is a polarity variable that determines if the feature f should be greater or smaller than the threshold in crater images. The output of each classifier depends only on a single feature. Therefore, the boosting algorithm selects a weak classifier (feature) in each round. The parameters of the weak classifiers are obtained by minimizing the criterion

$$E(f) = \sum_{i=1}^{N} w_i \left| h(B_i, p, \theta) - y_i \right| \tag{3}$$

where B_i is the ith training pattern, w_i is the corresponding weight (see its definition in the succeeding discussions), and $y_i \in \{0, 1\}$ is the correct decision ($y_i = 1$ for the crater training patterns and $y_i = 0$ for the noncrater patterns). This algorithm selects one feature per iteration. The main steps are briefly described in the following (see [16] for the details).

1) Extract all features f from each training block using (1).
2) Initialize the weight $w_{1,i}$ for each training block i

$$w_{1,i} = \begin{cases} \frac{1}{2 \cdot \mathrm{tc}}, & \text{if } i \text{ is crater} \\ \frac{1}{2 \cdot \mathrm{nc}}, & \text{if } i \text{ is noncrater} \end{cases} \tag{4}$$

   where tc is the number of true craters and nc is the number of noncraters in the training set.
3) For $t = 1, \ldots, T$ (T is the number of features to be selected), perform the following.
   a) Normalize the weights $w_{t,i}$.
   b) For each feature f, train the corresponding weak classifier by minimizing (3).
   c) Feature selection: Choose the weak classifier h_t with the lowest error $\varepsilon_t = \min_f E(f)$.
   d) Update the weights $w_{t,i}$

$$w_{t+1,i} = w_{t,i} \cdot \beta_t^{1-e_i} \tag{5}$$

   using $\beta_t = \varepsilon_t/(1 - \varepsilon_t)$; $e_i = 0$ if the training block i is correctly classified and $e_i = 1$ otherwise.
4) Combine the outputs of all the weak classifiers to obtain a discriminant function $H(B)$

$$H(B) = \sum_{t=1}^{T} \alpha_t \cdot h_t(B) \tag{6}$$

   where $\alpha_t = \log(1/\beta_t)$. The final decision $C(B)$ is obtained by computing the local maxima of $H(B)$ using a nonmaximum suppression algorithm. Accept or reject the local maxima by comparing $H(B)$ with a threshold as follows:

$$C(B) = \begin{cases} 1, & \text{if } H(B) \geq \mu \cdot \sum_{t=1}^{T} \alpha_t \\ 0, & \text{otherwise} \end{cases} \tag{7}$$

   where $\mu \in [0, 1]$ is a constant defined by the user, which defines the tradeoff between true and false detections.

III. Multiscale Classification

In order to detect craters of different sizes, the classifier should be scale independent. This problem has been addressed

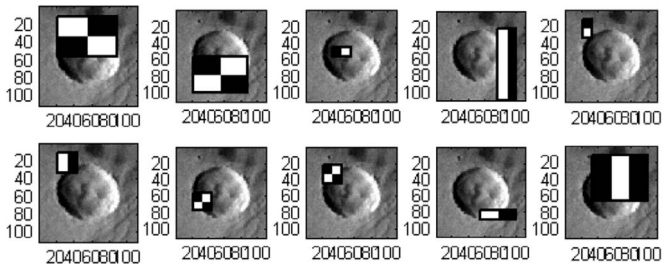

Fig. 3. First ten features selected with boosting over a crater.

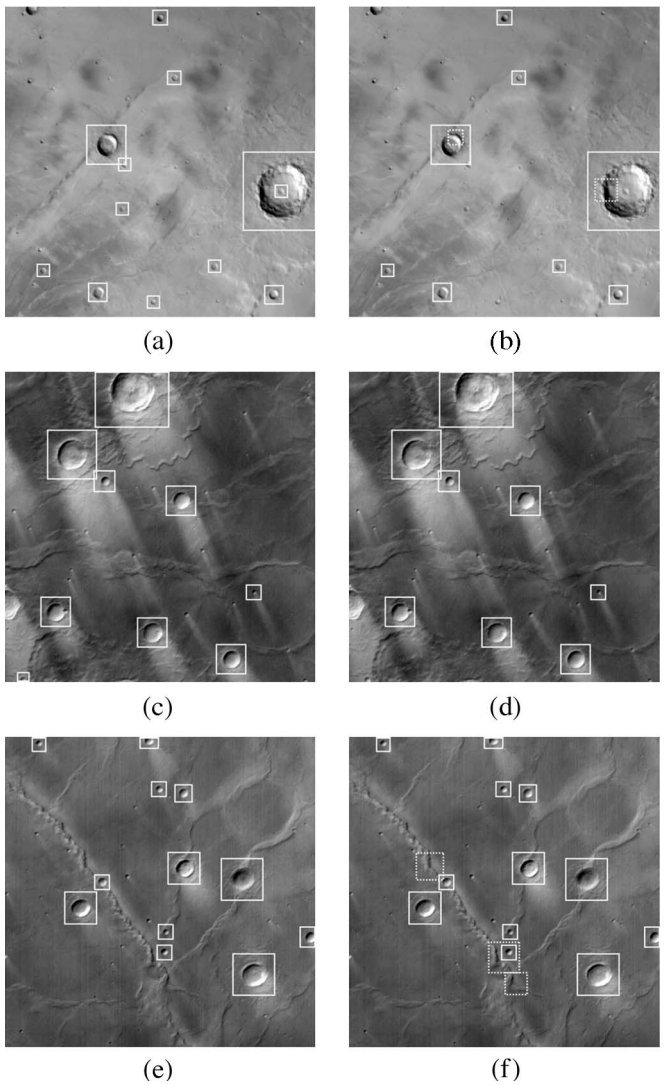

Fig. 4. Classification of MOC images E05-00815, E19-00650, and M00-03044: (a), (c), and (e) ground truth; (b), (d), and (f) classifier output (solid—correct detections; dashed—false detections) [image credits: NASA/JPL/MSSS].

before by several authors (see, e.g., [16] and [18]). The image is analyzed using blocks of different sizes $[0, K]^2$, with $K = 15 \times 1.25^{s-1}$ pixels, where s is the scale number. Each block is shifted by 1 pixel at a time with respect to the previous block. The number of features considering all scales is 3216 per block. In order to allow for the simultaneous use of the same

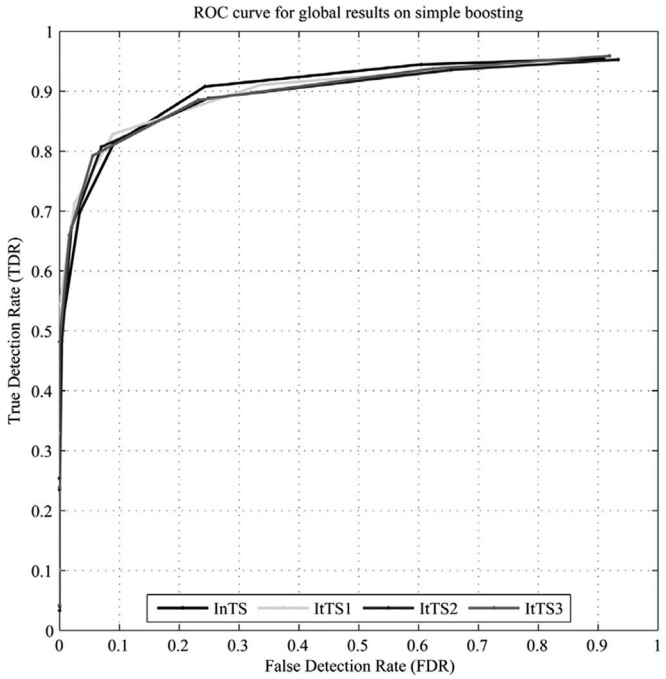

Fig. 5. ROC curve for different values of the threshold μ and different number of iterations of the training set.

classifier at different scales, the features are normalized to turn them scale independent

$$f(B) = \frac{1}{K^2} \int\limits_{[0,K]^2} B(x)\phi\left(\frac{x}{K}\right) dx. \tag{8}$$

To perform the detection of craters in an image, the outputs of the boosting classifiers at different scales must be compared. This way, we search for the local maxima of $H(B)$ in space $\times$ scale volume, i.e., we look for the locations and scale in which $H(B)$ achieves the highest values in a given neighborhood.

This means that the same classifier is used for all the scales considered in the classification procedure being trained with patterns (crater and noncrater blocks) of different scales. This situation is possible to attain since we are dealing with scale-independent features.

IV. Experimental Results

There is no standard procedure to evaluate crater detection algorithms, although very recent proposals are being presented to change that situation [19]. Many algorithms are evaluated in a specific way by the authors using their own metrics and data sets. In this letter, we use well-established metrics [true detection rate (TDR) and false detection rate (FDR)] together with a set of images which was already used in another study [5]. This set comprises 101 images obtained by the Mars Orbiter Camera (MOC) from four zones of Mars surface, covering about 1 500 000 km^2 and belonging to the Hesperian geological period. All the images were manually classified in order to produce the ground-truth information. The bounding boxes of all the craters were accurately specified by an expert.

TABLE I
CLASSIFICATION PERFORMANCES FOR DIFFERENT THRESHOLD VALUES

μ	InTS		ItTS1		ItTS2		ItTS3	
	TDR (%)	FDR (%)	TDR (%)	FDR (%)	TDR (%)	FDR (%)	TDR (%)	FDR (%)
0.55	94.48	60.47	91.09	33.71	88.82	24.83	88.55	23.20
0.60	90.79	24.29	82.82	8.88	80.70	7.01	79.24	5.53
0.65	81.07	8.93	71.25	2.51	67.24	1.98	67.03	1.91

Therefore, we know the exact location (contour, center, and diameter) of 1272 craters in the images.

A. Training Data

The algorithm was tested using fourfold cross-validation, i.e., the whole set of images was divided into four subsets with the same size; while three of them were used for training, the remaining one was used for testing. This procedure was repeated four times, so that each subset could be used once for testing.

The boosting classifier is trained using positive (crater) and negative (noncrater) examples extracted from the training database. The positive examples are obtained using all the craters in the training images. Each example is a square block centered on the crater with a size equal to 1.30 times its diameter. Some criteria to select the negative examples are needed, since there are too many possibilities for defining the noncrater blocks. We initially extracted negative examples occurring in the borders or rims of the craters, because they correspond to highly textured regions confounded with craters and which are hard to classify. Therefore, a small number of noncrater blocks are taken around each crater. This set of negative patterns is called the initial training set (InTS) which is used to train the initial classifier. Afterward, we found, in practice, that this approach was insufficient since it did not provide a representative collection of negative patterns.

Thus, in order to enlarge and enhance this set of noncrater examples, we enhanced the training set with additional blocks corresponding to the false detections with higher discriminant value and repeat the previous procedure. At each iteration, a new classifier is obtained trained with a larger data set. This enlarged set is called an iterative training set (ItTS). This procedure is repeated a few times until the improvement is negligible.

B. Boosting Classifier

Each training block is characterized by 3216 features. The boosting algorithm extracts a small subset of T features which are considered to be sufficient for the decision. In Fig. 3, the ten best masks selected by the boosting algorithm for a given training set are shown, together with a crater image. These masks show the kind of transitions which are considered the most relevant by the classifier. We considered several values of T ranging from 10 to 50 features in the experimental tests.

C. Evaluation

The performance of the boosting algorithm is evaluated through the computation of TDR and FDR, given by following expressions:

$$\mathrm{TDR}(\%) = \frac{\mathrm{TD}}{\mathrm{GT}} \times 100 \tag{9}$$

$$\mathrm{FDR}(\%) = \frac{\mathrm{FD}}{\mathrm{TD} + \mathrm{FD}} \times 100 \tag{10}$$

where GT is the total number of craters in the ground-truth image, TD is the number of true detections and FD is the number of false detections. Only the craters with a diameter equal to or greater than 7 pixels are taken into account to calculate the TDR values. The detections are automatically evaluated as true or false by comparison with the ground-truth images. Fig. 4 shows representative examples of detections obtained with the proposed approach in three images with distinct characteristics.

For all retrieved classifiers in the fourfold cross-validation, the tradeoff between the true detections and false alarms is given by a receiver operating characteristic (ROC) curve, which was built as a function of the classifier threshold μ on (7).

Fig. 5 shows the global ROC curves obtained from the mean of the four curves for the InTS and for three iterations of ItTS (ItTS1, ItTS2, and ItTS3). In particular, some of those values are presented in Table I for three different threshold values μ.

The results obtained are comparable with the best performances achieved so far by other methods since, for instance, we obtained with three iterations of ItTS a detection rate of 88.5% for 23.2% of false alarms. The higher the true detections are, the higher the false detections become.

Nevertheless, the inclusion of noncrater patterns into the training sets obviously leads to major improvements in the performance of false detections of about two to four times: For instance, for $\mu = 0.60$, the FDR value is reduced to about one-third when InTS is enlarged to ItTS1 (from 24.29% to 8.88%) or to about one-fourth using ItTS3 (FDR $= 5.53\%$).

The influence of the number of features used in the classification was also evaluated. It can be noticed that the performance of the classifiers increases with the number of features (iterations) used, i.e., the performance increases with the use of more features, like shown by the ROC curves in Fig. 6 for five different feature sizes (from 10 to 50).

V. CONCLUSION

This letter describes a boosting algorithm for impact crater detection which accounts for changes in illumination, visual appearance, and size. The algorithm was evaluated in an objective way using images from Mars related to the Hesperian period. The results obtained outperform most published approaches. Furthermore, this algorithm is computationally fast and also

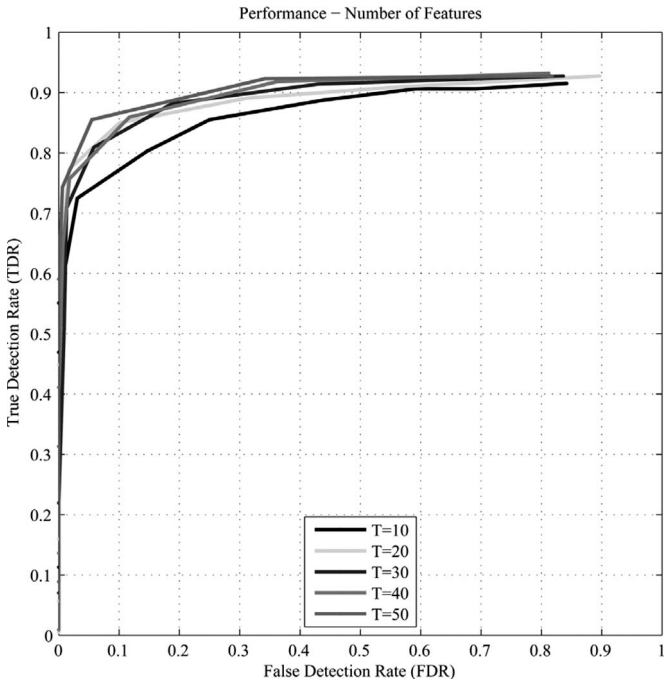

Fig. 6. ROC curve for different values of the threshold μ and different number of features (T).

diminishes the minimum detection limit of crater dimensions, i.e., it detects craters with a diameter equal to or greater than 7 pixels, a real and valuable improvement when compared to the limit of at least 10 pixels of other approaches.

The boosting algorithm is able to automatically select a small set of features characterizing the presence/absence of craters in an image. Thus, the major improvements introduced by this approach are its adaptive characteristics together with an original learning strategy, reflected on the robust performances achieved by cross-validation.

We believe that this approach can be applied to other types of terrains, since the boosting algorithm is able to automatically select meaningful features for each classification problem. Therefore, in the future, we plan to evaluate the performance of this algorithm on other terrains of Mars (namely, the older or Noachian ones) and also on other planetary surfaces.

REFERENCES

[1] W. K. Hartmann and G. Neukum, "Cratering chronology and the evolution of Mars," *Space Sci. Rev.*, vol. 96, no. 1–4, pp. 165–194, Apr. 2001.

[2] A. Flores-Méndez, *Crater Marking and Classification Using Computer Vision,* Lecture Notes in Computer Science, vol. 2905. Berlin, Germany: Springer-Verlag, 2003, pp. 79–86.

[3] G. Michael, "Coordinate registration by automated crater recognition," *Planetary Space Sci.*, vol. 51, no. 9, pp. 563–568, Aug. 2003.

[4] T. Barata, E. I. Alves, J. Saraiva, and P. Pina, *Automatic Recognition of Impact Craters on the Surface of Mars,* Lecture Notes in Computer Science, vol. 3212. Berlin, Germany: Springer-Verlag, 2004, pp. 489–496.

[5] L. Bandeira, J. Saraiva, and P. Pina, "Impact crater recognition on Mars based on a probability volume created by template matching," *IEEE Trans. Geosci. Remote Sens.*, vol. 45, no. 12, pp. 4008–4015, Dec. 2007.

[6] T. Vinogradova, M. Burl, and E. Mjolness, "Training of a crater detection algorithm for Mars crater imagery," in *Proc. IEEE Aerosp. Conf.*, Big Sky, MT, 2002, vol. 7, pp. 3201–3211.

[7] J. R. Kim, J.-P. Muller, S. van Gasselt, J. G. Morley, and G. Neukum, "Automated crater detection, a new tool for Mars cartography and chronology," *Photogramm. Eng. Remote Sens.*, vol. 71, no. 10, pp. 1205–1217, Oct. 2005.

[8] B. D. Bue and T. F. Stepinski, "Machine detection of Martian impact craters from digital topography data," *IEEE Trans. Geosci. Remote Sens.*, vol. 45, no. 1, pp. 265–274, Jan. 2007.

[9] A. A. Smirnov, "Exploratory study of automated crater detection algorithm," Boulder, CO, 2002. Tech. Rep..

[10] P. G. Wetzler, B. Enke, W. J. Merline, C. R. Chapman, and M. C. Burl, "Learning to detect small impact craters," in *Proc. 7th IEEE Workshops Appl. Comput. Vision WACV/MOTIONS*, vol. 1, 2005, pp. 178–184.

[11] S. Brumby, C. Plesko, and E. Asphaug, "Evolving automated feature extraction algorithms for planetary science," in *Proc. ISPRS WG IV/9: Extraterrestrial Mapping Workshop Advances-Planetary Mapping*, Houston, TX, 2003.

[12] C. Plesko, S. Werner, S. Brumby, E. Asphaug, and G. Neukum, "A statistical analysis of automated crater counts in MOC and HRSC data," in *Proc. 37th Lunar Planetary Sci.*, Houston, TX, 2006.

[13] E. R. Urbach, "Classification of objects consisting of multiple segments with application to crater detection," in *Proc. 8th ISMM*, Rio de Janeiro, Brazil, 2007, vol. 2, pp. 81–82.

[14] B. Leroy, G. G. Medioni, E. Johnson, and L. Matthies, "Crater detection for autonomous landing on asteroids," *Image Vis. Comput.*, vol. 19, no. 11, pp. 787–792, Sep. 2001.

[15] Y. Sawabe, T. Matsunaga, and S. Rokugawa, "Automated detection and classification of lunar craters using multiple approaches," *Adv. Space Res.*, vol. 37, no. 1, pp. 21–27, 2006.

[16] P. Viola and M. Jones, "Robust real-time face detection," *Int. J. Comput. Vis.*, vol. 57, no. 2, pp. 137–154, May 2004.

[17] C. Papageorgiou, M. Oren, and T. Poggio, "A general framework for object detection," in *Proc. 6th ICCV*, 1998, pp. 555–562.

[18] Y. Deng and G. Su, "Face detection based on fuzzy cascade classifier with scale-invariant features," *Int. J. Inf. Technol.*, vol. 12, no. 5, pp. 108–116, 2006.

[19] G. Salamunićcar and S. Lončarić, "Open framework for objective evaluation of crater detection algorithms with first test-field subsystem based on MOLA data," *Adv. Space Res.*, vol. 42, no. 1, pp. 6–19, 2008.